Antibody responses to Zika virus infections in flavivirus-endemic environments

Sarah L. Keasey[1,2], Christine L. Pugh[2], Stig M. R. Jensen[2], Jessica L. Smith[2], Robert D. Hontz[3,4], Anna P. Durbin[5], Dawn M. Dudley[6], David H. O'Connor[6], and Robert G. Ulrich[2,7*]

[1]Department of Biology, University of Maryland-Baltimore County, Baltimore, Maryland 21250 USA.

[2]Molecular and Translational Sciences Division, U.S. Army Medical Research Institute of Infectious Diseases, Frederick, Maryland 21702, USA.

[3]Naval Medical Research Center, Silver Spring, Maryland 20910 USA; U.S. Naval Medical Research Unit No. 6 (NAMRU-6), Lima, Peru.

[4]Current address: Naval Medical Research Center, Biological Defense Research Directorate, 8400 Research Plaza, Fort Detrick, Maryland 21701, USA,

[5]Center for Immunization Research, Johns Hopkins Bloomberg School of Public Health, Baltimore, Maryland 21205, USA.

[6]Department of Pathology and Laboratory Medicine, University of Wisconsin-Madison, Madison, Wisconsin 53705, USA.

[7]Virology Division, U.S. Army Medical Research Institute of Infectious Diseases, Frederick, Maryland 21702, USA.

*Corresponding author: robert.g.ulrich.civ@mail.mil

Abstract

Zika virus (ZIKV) infections occur in areas where dengue (DENV), West Nile (WNV), yellow fever (YFV), and other viruses of the genus *Flavivirus* co-circulate. The envelope protein (E) of these closely related flaviviruses induces specific long-term immunity, yet subsequent infections are associated with cross-reactive antibody responses that may enhance disease susceptibility and severity. To gain a better understanding of ZIKV infections against a background of similar viral diseases, we examined serological immune responses to ZIKV, WNV, DENV and YFV infections of humans and non-human primates (NHP). Using printed microarrays, we detected very specific antibody responses to primary infections with probes of recombinant E proteins from fifteen species and lineages of flaviviruses pathogenic to humans, while high cross-reactivity between ZIKV and DENV was observed with eleven printed native viruses. Notably, antibodies from human primary ZIKV or secondary DENV infections that occurred in flavivirus-endemic areas broadly recognized E proteins from many flaviviruses, especially DENV, indicating a strong influence of infection history on immune responses. A predictive algorithm was used to tentatively identify previous encounters with specific flaviviruses based on serum antibody interactions with the multi-species panel of E proteins. These results illustrate the potential impact of exposures to related viruses on the outcome of ZIKV infection, and offer considerations for development of vaccines and diagnostics.

Introduction

Zika disease is primarily spread to humans by transfer of Zika virus (ZIKV) through the bite of infected *Aedes aegypti* or *Aedes albopictus* mosquitoes (1, 2), and secondarily by sexual (3) or vertical (4-6) transmission. The majority of ZIKV infections are asymptomatic or mild with low-

grade fever, arthralgia, conjunctivitis, and rash (7), while a lower frequency of cases may result in congenital microcephaly via *in utero* infections in infants and Guillain-Barré syndrome in adults (4-6, 8). Prior to the first reported outbreaks in the Pacific Islands in 2007 (9) and 2013-2014 (10, 11), only sporadic human cases of ZIKV were documented in Africa and Southeast Asia (10, 11). However, the number of confirmed human cases has increased dramatically over the past nine years as ZIKV has spread to regions with naïve populations, leading to the current epidemic in Brazil and another 58 countries with on-going ZIKV transmission (12).

The single-stranded (+) genomic RNA of ZIKV and other *Flavivirus* species (flaviviruses) encodes a non-segmented open reading frame that is cleaved during and after translation into three structural proteins (capsid, C; envelope, E; membrane M) that are incorporated into the virus, and seven non-structural proteins (NS1, 2A, 2B, 3, 4A, 4B, 5) that are necessary for replication. The overall molecular organization of the mature ZIKV from cryo-EM structures (13, 14) is very similar to the closely related dengue (DENV) and West Nile (WNV) viruses (15, 16), as well as more distantly related tick-borne encephalitis (TBEV) and Japanese encephalitis (JEV) viruses (17, 18). However, infectious particles also exhibit structural heterogeneity from immature to mature forms (19) within species, which may affect the protective potency of antibodies. Heterodimers of E and M displayed on the outer surface of the virus (13, 14) undergo extensive conformational changes that facilitate infection of cells, and these proteins are primary targets for circulating antibodies. Further, the E protein of many flavivirus strains harbor a potentially glycosylated, four-residue loop, and deletions of this feature in ZIKV are selected against *in vivo* (20). The NS1 protein, which is secreted by infected cells (22), is another important antigen that may be involved in immune evasion and pathogenesis. The specificities

Clinical and Vaccine Immunology

of antibodies interacting with NS1 are likely to be affected by a balance of surface features that are conserved among flaviviruses as well as the diverse electrostatic characteristics (23).

The four DENV serotypes (DENV1-4) are loosely categorized by cross-neutralization with polyclonal antibodies (24). Serological immune responses protect from reinfection with the same (homotypic) virus, while cross-reactive antibodies generated from previous infections with another (heterotypic) DENV serotype may enhance disease outcomes (25-28). Although most infections are mild and self-limiting, dengue disease can progress to hemorrhagic fever, capillary leakage, and dengue shock syndrome (27, 28). Secondary heterotypic infection can in some cases lead to increased risk of severe dengue disease, possibly because antibodies to one serotype may enhance infections with heterologous serotypes (antibody-dependent enhancement or ADE) by promoting viral entry and infection through Fc receptor-expressing cells (27-30). The extent of disease enhancement in human ZIKV infections due to preexisting flavivirus antibodies is not well documented. While there is a higher risk of more severe disease from secondary DENV infections, among flaviviruses severe neurological pathologies may be uniquely associated with ZIKV infections during fetal development, with considerable uncertainty remaining regarding potential long-term health effects.

Beyond the potential role of antibodies in exacerbating disease, there are great challenges for developing accurate serological tests for ZIKV infections. Assays were recently developed and FDA-approved under Emergency Use Authorization for the detection of viral RNA or specific IgM and neutralizing antibodies in biological fluids of patients with suspected Zika disease (31, 32). However, negative results for viremia do not exclude ZIKV infection, as circulating virus levels are highest several days before symptom onset, and begin to decline early in the acute phase of infection (33). In addition, interpretation of ZIKV antibody test results is

Clinical and Vaccine Immunology

68 complicated due to suspected cross-reactivity with other flaviviruses, especially for individuals
69 who have had previous flavivirus exposures. Infections caused by DENV, WNV, and yellow
70 fever (YFV) viruses are spread by common mosquito vectors, circulate in similar areas, and
71 present early disease symptoms that are identical to ZIKV infections (25-28). Infected
72 individuals may have high levels of antibodies to multiple flaviviruses that hinder conclusive
73 determination of the virus responsible for the most recent infection (29). Thus, laboratory
74 methods that can better differentiate clinical infections and facilitate accurate disease
75 surveillance are integral to an effective public health response to the current Zika disease
76 epidemic and to future outbreaks. Towards this goal, we examined serological immune responses
77 to commonly encountered infections by using a microarray of viruses and isolated protein
78 antigens representing major phylogenetic lineages of flaviviruses. Our results demonstrate that
79 primary human and rhesus macaque antibody responses to infection are highly specific for
80 envelope proteins from the etiological agent, while responses to whole viruses are most cross-
81 reactive. We further show that antibody recognition of isolated viral antigens can be used to
82 resolve complex infection histories.
83
84 **Materials and Methods**
85 **Viruses.** The ZIKV and DENV presented in Table 1 were propagated and prepared as previously
86 described (34), with some modifications. Briefly, HEK293T cells, were maintained in DMEM,
87 supplemented with 10% FBS, at 37°C and 5% CO_2. Cells were seeded in T125 flasks to 60%
88 confluency and cultured for 12 h. The cells were infected (2 h) with 5 ml of suspended virus
89 stock diluted 1:25 with fresh culture media. Infectious suspensions were replaced for virus
90 propagation, and culture supernatants were harvested at early (48 h) and late (144 h) time points

to obtain immature and mature virions, respectively, while adding fresh HEK293T cells 72 h post-infection (to yield 60% confluency 1/11 of a confluent 3-layer T125 flask) to ensure the presence of enough viable cells for sustained proliferation to generate mature virus. Culture supernatants were filtered using pre-washed (Super G blocking buffer (Grace Bio-labs) followed by sterile PBS) 45 µm syringe filters, and precipitated for 12 h (4°C) in 8% PEG8000 in PBS (v/v). Precipitates of viruses were pelleted by centrifugation (14,000 x *g*, 1 h, 4°C), resuspended in 300 µl sterile PBS (~100-fold concentration by volume), snap-frozen in a dry-ice/ethanol bath, and stored at -80°C.

Viral proteins. Viral RNA for preparation of protein-expression plasmids were obtained from the following sources: American Type Culture Collection© (DENV1-4), Integrated BioTherapeutics, Inc.© (YFV and Japanese encephalitis virus (JEV)); NIAID-World Reference Center for Emerging Viruses and Arboviruses (Dr. Robert Tesh) (St. Louis encephalitis virus (SLEV), WNV, and rocio virus (ROCV)). The cDNA templates of E, NS1, and pM genes were produced by reverse transcription of full-length viral RNA by using 50 µM Oligo(dT)$_{20}$ primers and the SuperScript® III Reverse Transcriptase First-Strand Synthesis System (Life Technologies). ZIKV genes (E, NS1, pM) and E genes from Murray Valley encephalitis virus (MVEV), Powassan virus (POWV), and tick-borne encephalitis virus (TBEV) were synthesized (gblocks®, Integrated DNA Technologies, Inc; GeneStrings, Life Technologies), with codon optimization for expression in *Escherichia coli*. Synthesized genes and cDNA were used as templates in PCR amplification reactions (50 µL total) with gene specific primers (final 2.5 µM conc.) and 2X Phusion High-Fidelity PCR master mix with HF buffer (New England BioLabs Inc.®). PCR amplified genes were purified using QIAquick spin column PCR purification kit

(QIAGEN). NS1 and pM were produced as full-length open reading frames (ORFs), and E genes were truncated to exclude transmembrane domains, as predicted by analysis of amino acid sequences using TMHMM Server v.2.0 (Center for Biological Sequence analysis) (35, 36). Purified DNA were TOPO® cloned into the pENTR™/TEV/D-TOPO® vector (Gateway® Technology, Life Technologies™). Sequence-verified entry clones were shuttled into expression vectors by recombination reactions using LR clonase II (Life Technologies). Specifically, the ZIKV-MR766-pM ORF was shuttled into an N-terminal His-maltose-binding protein (HisMBP) tagged vector (37), while all other flaviviral ORFs were shuttled into the N-terminal 6XHis tagged pDEST17 (Life Technologies). All flavivirus constructs were expressed in *E. coli* BL21(DE3), propagating bacteria in media containing Luria broth (300 ml) supplemented with 100 µg ml^{-1} ampicillin and 0.1% glucose. Proteins were induced at mid-log phase with 1 mM isopropyl-beta-D-thiogalactopyranoside (IPTG, EMD Chemicals). Induction conditions were optimized for each protein, and bacteria were grown at either 30°C (2-4 h) or 18°C (12 h) prior to harvest by centrifugation. Bacterial pellets were lysed in B-PER reagent (Thermo Scientific) containing EDTA-free 3x Halt™ Protease Inhibitor Cocktail (Thermo Scientific), 0.2 mg ml^{-1} lysozyme, 250 U DNase I (Thermo Scientific), and 1 mM IPTG. Protein expression was analyzed by SDS-PAGE (Bio-Rad) followed by Coomassie stain, and Western blot using a mouse anti-His-HRP conjugated polyclonal antibody (Abcam). For purification of insoluble proteins, inclusion body pellets were washed as previously described, with minor modifications (38). Briefly, buffer containing 50 mM Tris-HCl pH 7.4, 1 M urea, and 1% Triton X-100 was used to wash pellets 3 times, followed by 2 washes with Tris-HCl pH 7.4, with centrifugation at 15,000 x *g* for 7 min between each wash, and purified pellets were stored at -80°C. Purified inclusion bodies were solubilized in 50 mM HEPES pH 7.3, 140 mM NaCl, 2 mM DTT, and 1%

Clinical and Vaccine Immunology

sodium dodecyl sulfate (SDS), followed by incubation at 99°C with gentle mixing (5-15 min), and centrifugation to remove remaining insoluble protein. Solubilized proteins were analyzed by SDS-PAGE electrophoresis with Coomassie Blue staining, and by Western blotting using anti-His-HRP conjugated polyclonal antibody (Abcam). Protein concentration and purity of flavivirus proteins were measured using the Agilent Protein 230 kit and Bioanalyzer 2100 instrument (Agilent Technologies). Purified proteins were stored at -20°C in solubilization buffer, with a final 25% glycerol concentration.

Microarrays of flavivirus antigens. Recombinant proteins were diluted to 200 ng μl^{-1} in microarray printing buffer (50 mM HEPES, 140 mM NaCl, 2 mM DTT, pH 7.3) with glycerol added to a final concentration of 40%. Flavivirus and control proteins were printed onto microporous nitrocellulose-coated slides (ONCYTE® SuperNOVA, Grace Bio-labs, Inc) in replicates (n = 6) using a non-contact inkjet microarray printer (ArrayJet, Glasgow, UK). The virus preparations were printed with printing buffer containing 50% glycerol, and preliminary experiments were performed with printed virus to optimize antibody binding signals. Frozen virus stocks were gamma-irradiated (6 Mrad) for inactivation and visualized by electron microscopy to assess quality and quantity. Concentrated virus and a dilution series of bovine serum albumin (BSA; Sigma-Aldrich) were subjected to SDS-PAGE, and stained with Coomassie Blue to determine the relative amount of viral proteins in each preparation. The final printing parameters were established by comparison of virus gradients printed onto nitrocellulose-coated slides, where deposited material was quantified against both an IgG and a BSA standard gradient by SYPRO®Ruby staining, and by comparing signal strength with a pan-flavivirus polyclonal rabbit antiserum specific to an E-domain II peptide that is highly conserved

among flaviviruses. The deposited protein antigens were similarly evaluated using SYPRO®Ruby, an anti-N-terminal 6XHis monoclonal antibody (Sigma Aldrich), and the pan-flavivirus rabbit antisera described above. Printed microarrays were desiccated (12 h) and stored frozen (-20^{o}C) until use.

Microarray assays. All microarray processing steps were performed at 22^{o}C, protected from light. For IgM detection assays, serum IgG was inactivated using GullSORB^{TM} (Meridian) prior to performing microarray manipulations. NHP (1:50) and human (1:150) sera, diluted in probe buffer (1µ PBS pH 7.4, 0.1% Tween 20, 1% BSA), were precleared by incubating (1 mg ml^{-1}) with *E.coli* lysate (Promega) with gentle agitation, followed by centrifugation (17,000 x *g*, 5 min) to remove the pelleted immunoprecipitates. Microarrays were blocked with Super G blocking buffer (Grace Bio-labs) for (1.5 h, 22^{o}C) and washed 3 times (5 min each) in wash buffer (1x PBS, 0.2 % Tween® 20, 1% BSA). The microarrays were incubated (2 h) with *E. coli*-cleared serum, washed (5x, 5 min each), and incubated (1 h) with either goat anti-human γ-specific IgG (1:1000) or goat anti-human µ-specific IgM (1:250) Alexa Fluor 647-conjugated secondary antibody (Southern Biotech) diluted in probe buffer. Microarrays were washed 3x with wash buffer, rinsed twice with filtered deionized water to remove any residual salts, and dried.

Data acquisition and analysis. Microarray slides were scanned at 635 nm using a confocal laser scanner (GenePix® 4400A scanner; Molecular Devices) using settings below signal saturation. Background-subtracted pixel counts were determined with GenePix® Pro 7 software, and outliers among data replicates, identified using a modified Z-score (median absolute deviation >3.5), were removed. Pixel counts from replicate spots were averaged to obtain mean

Clinical and Vaccine Immunology

fluorescence intensity (MFI) and used for subsequent analyses. Relative binding was calculated as

$$RB = (x / x_i)100,$$

where x is MFI originating from microarrayed antigens, and i is the infecting virus species. Relative binding signals were used in hierarchical clustering analyses (average-linkage Pearson correlation) performed using MeV v4.8.1 within the TM4 software suite (39). Student's t-tests, polynomial curve fitting, principal component analyses, and one-way analysis of variance (ANOVA) with Tukey's post-hoc honest significant difference (HSD) test were performed using OriginPro v9.0 (Origin Lab Corporation).

Machine learning. The support vector machine (SVM) method LIBSVM (http://www.scie.ntu.edu.tw/~culin/libsvm/), available in the R package e1071 (40), was used for predictions of infection histories with quantile normalized microarray data. An optimal separating hyperplane between data classes was determined with the SVM by maximizing the margin between closest points and minimizing the classification error. All binary subclassifiers were fitted to the model, and the correct class was identified by a voting mechanism (i.e. the class with the highest probability). We used a radial basis function (RBF) as the kernel function, which is defined by

$$K(u,v) = \exp(-\gamma||u-v||^2),$$

where u and v are two data vectors and γ (set to 0.001) is a training parameter that makes the decision boundary smoother as the value becomes smaller. The regularization factor C, set to 100, controls trade-off between a low training error and a large margin. A grid search was used for selection of C (1 - 1000) and γ (0.0001 – 1) using 10-fold cross-validation of the training

dataset and the built-in "tune" function of e1071. The final SVM model was generated using the optimal parameters with complete training datasets. To evaluate the model performance, a 10-fold cross validation was implemented on the training dataset, which consisted of a positive set of E-specific antibody binding signals from primary flavivirus infections (n = 32, human and NHP) and a negative set of background signals from flavivirus-naïve sera (n = 34, human and NHP). Based on one-way ANOVA followed by Tukey's range test, the overall antibody binding patterns of DENV2-challenged NHPs and humans were not statistically different ($p > 0.05$). Therefore, the positive training set consisted of data from both rDEN2Δ30-challenged humans and NHPs. The training dataset was randomly divided into ten equal parts, and each run of cross-validation was comprised of 1/10 as the independent test dataset and the remaining 9/10 as the training dataset. The performance of the model was calculated as *accuracy = (TP +TN) / (TP+FP+TN+FN).*

E protein molecular phylogeny. A phylogenetic tree was generated based on E amino acid sequences (Asian-YAP/2007 and African-MR-766/1947 -lineage ZIKV selected as representative strains). CLUSTAL W2 (41) was used to generate three multiple sequences alignments (MSAs), each with a different gap opening penalty (5, 10, 25), Blosum62 as the protein weight matrix, and all other options left as default. T-Coffee Combine (42, 43) was then used to generate a single alignment that had the best agreement of all three MSAs. Gblocks (44, 45), with relaxed settings (small blocks allowed, gap positions allowed within final blocks, and less strict flanking positions), was used to eliminate poorly aligned positions and divergent regions in the combined alignment, and 202 conserved columns within the alignment were retained. A molecular phylogeny was generated using the maximum likelihood method implemented in the PhyML

program (v3.0 a LRT) (46). The Blosum62 substitution model and 4 gamma-distributed rate categories were selected to account for rate heterogeneity across sites. The gamma shape parameter was estimated directly from the data (γ= 1.564). Tree topology and branch length were optimized for the starting tree and subtree pruning and regrafting selected for tree improvement.

Animal and human sera.

Animal use statements.

All macaque monkeys used in this study were cared for by the staff at the Wisconsin National Primate Research Center (WNPRC) in accordance with the regulations and guidelines outlined in the Animal Welfare Act and the Guide for the Care and Use of Laboratory Animals and the recommendations of the Weatherall report (http://royalsociety.org/topics-policy/publications/2006/weatherall-report/). This study was approved by the University of Wisconsin-Madison Graduate School Institutional Animal Care and Use Committee (Animal Care and Use Protocol Number G005401). For all procedures (i.e., physical examinations, virus inoculations, ultrasound examinations, blood and swab collection), animals were anesthetized with an intramuscular dose of ketamine (10 ml kg^{-1}). Blood samples were obtained using a vacutainer system or needle and syringe from the femoral or saphenous vein.

Human use statements.

Research on human subjects was conducted in full compliance with DoD, NIH, federal, and state statutes and regulations relating to the protection of human subjects and adheres to principles identified in the Belmont Report (1979). All specimens, data, and human subject research were gathered and conducted for this publication under IRB-approved protocols.

Clinical and Vaccine Immunology

252

253 **ZIKV**. Three groups of Indian origin *Macaca mulatta* (3 individuals per group) were challenged
254 subcutaneously with a different dose (10^6, 10^5, or 10^4 plaque forming units (PFU)) of either an
255 Asian (Study ID ZIKV001 and ZIKV004) or African (Study ID ZIKV002) -lineage ZIKV (Table
256 1, Supplementary Fig. 1A). Sera were collected prior to ZIKV challenge (day 0) and daily for 10
257 days (all cohorts), followed by two to three times a week from 11 to 28 days post-infection (DPI)
258 (ZIKV001 and ZIKV002 only) (33, 47) (https://zika.labkey.com). Human sera from ZIKV
259 infections were collected from four female patients from the Dominican Republic that developed
260 symptoms of ZIKV (fever, joint pain, headache, conjunctivitis, rash, and muscle pain) in January
261 2016 (Supplementary Fig. 1C). Three patients were PCR confirmed for ZIKV infection by the
262 CDC within the first two weeks of symptom onset, whereas the remaining patient tested positive
263 for the presence of anti-ZIKV IgG by a microplate ELISA assay (EUROIMMUN, Inc.), as
264 performed by BocaBiolistics (Pompano Beach, FL), and sera were collected at 12-31 days post-
265 symptom onset.

266

267 **DENV.** Sixteen healthy, flavivirus naïve rhesus macaques (*M. mulatta*) were subcutaneously
268 injected with 10^5 PFU of either DENV1 (West Pac 74), DENV2 (S16803), DENV3 (CH53489),
269 or DENV4 (341750) (n=4 per challenge group, Supplementary Fig. 1A and 4), derived from low
270 passage, near wild-type virus isolates. Sera were collected prior to and 30 DPI (48, 49). Sera
271 from human primary DENV2 infections (n = 10, Supplementary Fig. 1B) were collected as part
272 of a DENV human challenge model originally developed by the Laboratory of Infectious
273 Diseases at the U. S. National Institutes of Health. Sera from participants that had no prior
274 history or serological evidence of flavivirus infection were collected prior to and 28 day post-

challenge with 10^3 PFU of rDEN2Δ30. rDEN2Δ30 induced viremia in all participants by 5 DPI (50, 51). Two individuals exhibited elevated binding to flavivirus E prior to challenge with rDEN2Δ30 (Supplementary Fig. 4) and were further excluded from our analysis. Convalescent DENV sera (n=7) were collected in Peru by the U.S. Naval Medical Research Unit No.6 (NAMRU-6) between February 2011 and November 2013. Subjects had febrile illness for five days or less and were confirmed to have DENV infections (DENV2, n=5; DENV3, n=2; Supplementary Fig. 1C) by PCR during the acute phase of infection. Sera were collected 14-24 days after confirmation of acute infection.

YFV. Early-Immune Yellow Fever Virus Antisera from three NHPs (Supplementary Fig. 1A; NR-29335, 29337, 29338; BEI Resources, NIAID, NIH), immunized by subcutaneous injection of 0.5 mL of live, attenuated YFV vaccine (strain 17D (52)), were collected 30 days after vaccination. Human sera from 17D-vaccinated individuals (seven primary and six boosted, Supplementary Fig. 1D), collected 14 – 118 after vaccination, were obtained from the Department of Defense Serum Repository (Silver Spring, MD).

WNV. Confirmed WNV-infected human sera (n=20, Supplementary Fig. 1D) were collected between 2009 and 2011 at FDA approved blood donor locations within the U.S., in accordance with a surveillance protocol performed by the National Heart, Lung, and Blood Institute (NHLBI) Biologic Specimen and Data Repository Information Coordinating Center (BioLINCC) (53). Sera were identified as WNV positive by nucleic acid testing, indicating a current WNV infection at the time of blood donation. WNV positive donors were then contacted for study enrollment, at which point subjects completed symptom questionnaires and provided subsequent

Clinical and Vaccine Immunology

blood samples at several weekly and monthly visits post-initial donation. Each specimen tested positive for the presence of WNV-specific IgM and IgG antibodies (54).

Control Sera. Sera collected by SeraCare Life Sciences, Inc. from healthy U.S. donors (n=5) were used for negative controls. These sera were selected based on no detectable antibodies to human immunodeficiency virus type 1 and type 2, Hepatitis A, B, and all flaviviruses used in the microarray.

Results

Antibody responses to ZIKV

To examine serological immune responses, we developed a flavivirus-focused microarray comprising mature and immature forms (34) of DENV1-4, and ZIKV (five Asian and six African lineage), along with recombinant protein antigens from fifteen isolates (Table 1, Fig. 1A). Equivalent densities of recombinant proteins or viruses, respectively, were deposited by ink-jet printing on microarray surfaces coated with a thin layer of nitrocellulose. The printed antigens were evaluated with mouse anti-sera against twelve flaviviruses, representing antibodies produced by a non-infectious route. The E antigens from all flaviviruses except DENV3 were detected by mouse antibodies (IgG) that were produced in response to the corresponding virus, as shown in Fig. 1B, with evidence of significant E cross-reactivity for JEV antisera. The NS1 proteins from all except DENV1-4 were detected by the mouse anti-virus sera, whereas the M antigen was only weakly recognized at best. We utilized the microarray to examine sera from NHPs (*M. mulatta*) that were challenged subcutaneously with either African or Asian isolates of ZIKV (Table 1; Supplementary Fig. 1A) (33, 47). The African and Asian lineages of ZIKV share

Clinical and Vaccine Immunology

~95% of E protein amino-acid sequences (55), or about the same level of similarity found among E proteins of individual DENV serotypes. Serum antibody binding to virus particles and E antigens of ZIKV, as measured by the microarray, was substantially elevated (Fig. 2A, B) 21-28 days post-infection (DPI), while no antibody recognition was observed for NS1 or M proteins (Fig. 2B), suggesting that anti-NS1 and -M antibodies represent a small proportion of the humoral immune response to infection during the time points examined. Antibody recognition was more robust for mature (~2-fold higher) compared to immature virus particles, which may display different conformations of E and M proteins (13). Within the assay, the highest antibody interactions were detected by ZIKV E proteins in comparison to mature ZIKV (Fig. 2A, B). However, a direct quantitative relationship between virus and recombinant protein cannot be determined by these results because the complex nature of the native virus precludes printing of equal molar amounts of available antigen. Only minor differences were observed in antibody responses to individual African and Asian-lineage ZIKV antigens for both virus and E (Fig. 2), consistent with the conserved amino acid sequences and a single ZIKV serotype, as recently reported by others (56). The E-specific IgM responses were detectable by 3 DPI, coinciding with the rise of virus, peaked by 11 DPI, and subsided thereafter (Fig. 2C). Corresponding IgG responses were delayed compared to IgM, consistent with a naïve immune response, and displayed increasing levels through 28 DPI (Fig. 2C). Specific IgG interactions were greater with E than virus for these assay results (Fig. 2C). Further, there were no apparent differences in the magnitude or kinetics of humoral immune responses to the different amounts of virus used for challenges (Supplementary Fig. 2), suggesting that levels of IgG and IgM were increasing in tandem with virus replication.

Cross-reactivity of antibodies from primary flavivirus infections

The E proteins of ZIKV and DENV have a high degree of structural similarity that may contribute to shared antibody epitopes. We examined NHPs (*M. mulatta*) challenged independently with DENV1-4 (Supplementary Fig. 1A) (48). For virus, antibodies (30 DPI) from NHPs infected with any DENV serotype were highly cross-reactive to heterologous DENV serotypes and ZIKV (Fig. 3A, Table 1). Further, DENV2 and 3 antibodies displayed substantially higher reactivity with the heterologous ZIKV, while IgG from ZIKV-challenged NHPs was more specific for ZIKV at the virus level, with a lower overall level of cross-reactivity towards DENV1-4 (Fig. 3A). In contrast with viruses, the E proteins presented antibody recognition profiles that were very specific for the challenge virus (Fig. 3A), and minimal antibody recognition of E proteins from ten more distantly related flaviviruses (Fig. 4A). DENV-challenged NHPs exhibited the highest antibody binding to the E protein from the DENV challenge serotype, and antibodies from ZIKV-challenged NHPs essentially bound only to ZIKV E antigens. A principal component analysis (PCA) of antibody bound by DENV and ZIKV E antigens differentiated serotype-specific DENV and ZIKV infection sera due to the higher degree of homotypic E recognition (Fig. 3B). In contrast to the E antigen results, PCA based on IgG recognition of virus only enabled distinction of ZIKV- from DENV-challenged sera, whereas DENV serotype-specific clusters were not evident (Fig. 3B). Furthermore, antibodies from NHPs challenged with African or Asian-lineage ZIKV were not differentiated by E or virus (Fig. 2, 3B). We also considered YFV, both as a nearest neighbor of ZIKV and DENV (Fig. 1A), and because vaccination against yellow fever is common in many countries with high dengue prevalence. While serum antibodies from NHPs vaccinated with the 17D YFV strain (Supplementary Fig. 1A) (52) predominantly recognized the E antigen of YFV (Fig. 4A), a

367 modest level of cross-reactivity was evident with several other E, including those of ZIKV and
368 TBEV.

369 The animals in the ZIKV, DENV, and YFV infection studies we examined were captive-
370 raised in isolation from most infectious diseases. Therefore, it was important to compare results
371 from the naïve backgrounds of animal disease models with primary infections of humans without
372 documented prior exposures to flaviviruses. Dengue human infection models were recently
373 developed to assess the efficacy of live attenuated DENV vaccines (50). Human challenges with
374 the attenuated DENV2 strain rDEN2Δ30 (51) result in a mild disease, with viremia, rash, and
375 neutropenia. We examined sera collected from flavivirus-naïve subjects 28 days after challenge
376 (10^3 PFU) with rDEN2Δ30 by subcutaneous injection (Supplementary Fig. 1B) (51). Among the
377 extended panel of E proteins (Table 1), human antibody responses to rDEN2Δ30 resulted in
378 specific recognition of the E protein from DENV2 and to a lesser degree DENV4 (Fig. 4A,
379 Supplementary Fig. 3A), which is most similar to DENV2 among all other flaviviruses (Fig. 1A).
380 Low levels of neutralizing antibodies against other DENV serotypes were previously reported for
381 individuals challenged with rDEN2Δ30 (57). For viruses, extensive human antibody cross-
382 reactivity was again noted for other DENV serotypes and ZIKV strains (Supplementary Fig. 3A).
383 These results indicated that the NHP DENV challenge model replicated the antigen-specificity
384 profile of human antibody responses to primary infection.

385 Antibody cross-reactivity between flaviviruses could be influenced by homology of
386 sequences and structures, as well as the abundance and degree of cross-reactive antibodies in
387 polyclonal sera. For example, cross-reactivity could be due to a small population of antibodies
388 that exhibit high levels of specificity for heterologous E proteins, or may be due to a larger
389 population of antibodies that exhibit broad cross-reactivity. Although the highest recognition of

the homologous E protein was common for antibodies from primary infections, we observed differences in the amount of total antibody across virus species (Fig. 5). Comparing results obtained with all E proteins, cross-reactive antibodies were undetectable for ZIKV, while DENV1 and DENV2 antibodies recognized other DENV serotypes. Antibodies from DENV3-infected and YFV-vaccinated NHPs exhibited the lowest binding to the respective E proteins, while a high level of DENV2 E-specific antibodies interacted with the DENV2 E protein (Fig. 5). The lower amount of DENV3 and YFV antibodies that were specific for the cognate E protein, compared to DENV2 for example, contributed to the appearance of an overall higher level of background cross-reactivity (Fig. 3A and 4A). Vaccination with the live-attenuated 17D strain results in low levels of viremia that mimic a true YFV infection and lower titers of specific antibodies compared to wild-type YFV infections (58). In addition, antibodies from NHPs challenged with ZIKV (33) and DENV (49) exhibited neutralizing antibody titers (33, 49) that directly correlated ($R^2 > 0.99$) with the E antibody recognition pattern we observed (Fig. 5). We concluded from these collective results with E proteins that the humoral immune response to primary flavivirus infections is surprisingly specific.

Secondary flavivirus infections

The antibodies of flavivivirus-naïve NHPs and humans to primary flavivirus infection were highly specific to the E protein of the challenge virus. Because increased levels of antibody cross-reactivity would be expected for flavivirus-primed individuals with secondary flavivirus infection, we next examined human sera after one or more flavivirus exposures. In contrast to results obtained with primary infections, IgG from DENV2 or DENV3 infections occurring in Peru prior to the Zika epidemic (here defined as secondary DENV infections; Supplementary

Fig. 1C) collectively interacted with several E proteins, including those from ZIKV (Fig. 4B), suggesting that antibodies from previous infections, possibly DENV4 (based on the amount of IgG bound), dominated immune responses to other flaviviruses. Despite expectations, sera from secondary DENV2 infections did not correlate with primary DENV2 infections (Supplementary Fig. 3B), providing additional evidence of previous dengue infection in these samples. Moreover, although principally recognizing the E protein of YFV, antibodies from human 17D vaccinations (Supplementary Fig. 1D) were less specific compared to those from primary NHP vaccinations, as E from DENV4 and several other flaviviruses were also targeted (Fig. 4B). It is possible that the less specific YFV responses were a result of declining antibody titers, as the sera were collected up to 118 days after vaccination. We further noted that serological responses from WNV infections that occurred in North America (Supplementary Fig. 1D), a region with only a small incidence of dengue, exhibited elevated antibody interactions with E from WNV and a few other flaviviruses, but only a low level of interactions with DENV antigens (Fig. 4B). Finally, we examined primary ZIKV infections from the Dominican Republic (Supplementary Fig. 1C), a dengue-endemic Caribbean country. Antibodies from ZIKV infections interacted to a greater extent with E proteins from DENV compared to ZIKV (Fig. 4B and Supplementary Fig. 3A), and also recognized E proteins from several other flaviviruses. It is important to note that levels of total E-specific antibodies from all human flavivirus exposures were significantly reduced compared to levels observed in primary infections (Fig. 5). While maximum E-specific antibody abundance never exceeded the low levels of binding observed for primary YFV and DENV3 exposures, these results suggested that serum levels of anti-E antibodies were predominantly driven by infection histories, and it is conceivable that at least one DENV infection preceded each clinical disease examined with sera from secondary infections.

Clinical and Vaccine Immunology

Given the complexity of the human antibody response from primary ZIKV and secondary DENV infections (Supplementary Fig. 1C), we attempted to estimate both the probability of previous flavivirus exposures and to identify the likely antecedent virus. We used a supervised machine learning method to classify sera by features of antibody binding to the extended panel of fifteen E proteins (Table 1). The support vector machine (SVM) classifier was trained on a positive set of E-specific antibody binding signals from primary flavivirus infections and a negative set of background signals from flavivirus-naïve sera. The performance of the SVM was evaluated using a 10-fold cross-validation re-sampling method, which readily differentiated infected from naïve sera and different primary infections, resulting in a total model accuracy of 98.5%. Using a probability cutoff value of ≥ 0.5, the classifier was used to predict flavivirus exposures that occurred prior to the secondary DENV and ZIKV infections. Four secondary DENV2 sera were predicted to have had a previous DENV4 infection, while high probability for two primary ZIKV sera suggested a previous DENV1 infection (Fig. 4C), which was consistent with clustering based on correlated antibody binding (Supplementary Fig. 3B). Lower overall probabilities for single virus infections were observed for the remaining secondary DENV and ZIKV samples, and classification to a single group was therefore not possible (Fig. 4C). For example, a secondary DENV3 serum had comparable probability values for DENV2 (0.28) and DENV4 (0.27), respectively, suggesting a previous infection with either virus. The inclusion of more extensive training data sets for primary ZIKV and other viral infections will be important for refining the predictive power of the described SVM method.

Clinical and Vaccine Immunology

459 **Discussion**

460 The coincidence of dengue in Zika epidemic areas limits the reliability of current serological
461 assays and complicates vaccination strategies. The study described here examined the specificity
462 of humoral immune responses to flaviviruses by using microarrays of eleven native viruses and
463 recombinant E proteins from fifteen species or lineages of flaviviruses that are pathogenic to
464 humans. Antibodies from first exposures of non-human primates and humans to ZIKV, DENV,
465 WNV, and YFV were predominantly directed towards the E surface antigen from the infecting
466 virus, and enabled differentiation of infections. Whereas isolated human monoclonal antibodies
467 that were cross-reactive for E antigens have been described (59), our results with polyclonal
468 antibodies present a global analysis of the composite B-cell response. In contrast to the high
469 specificity observed with E antigens, whole viruses exhibited significant levels of cross-
470 reactivity with serum antibodies from primary ZIKV and DENV infections. Antibodies from
471 human ZIKV or DENV infections that occurred in dengue-endemic regions recognized
472 heterotypic E antigens, and decreased recognition of the homotypic E, consistent with higher
473 levels of IgG from previous flavivirus exposures compared to the most recent infection. The
474 high degree of antibody specificity for E with sera from primary DENV and ZIKV exposures
475 suggests that the apparent cross-reactivity observed in many assays may result from an overlap in
476 rising and waning antibody responses to independent infections, as modeled in Figure 6. The
477 interpretation of serological results is further complicated by the lower antibody titers in Zika
478 disease compared to dengue, perhaps because serum ZIKV loads are also very low (60).

479 Clinical management of suspected Zika cases that test negative for viral RNA can be guided
480 by laboratory evidence of ZIKV-specific antibodies (32), particularly to differentiate infections in
481 late convalescence and beyond, as viral RNA is typically no longer detectable. Yet, results from

some *in vitro* assays will be difficult to extrapolate to human cases. Only weak antibody neutralization of ZIKV was reported for sera from DENV-infected patients that exhibited a high degree of cross-reactivity with ZIKV-infected Vero cell lysates (61), while other studies observe enhancement of ZIKV infections in cell culture by anti-DENV antibodies (59). Our results illustrate the application of high-throughput antigen microarrays for the study of antibody responses to ZIKV and other flaviviruses. In addition, printed microarrays provide a high-throughput means for evaluating the performance of many test antigens in the same assay. For example, by including both recombinant proteins and viruses in the same microarray, we determined that E proteins were the most effective probes for detecting serological immune responses. In agreement with previous reports that used antigen preparations from whole virus (9, 31)(61), we observed a high level of antibody cross-reactivity between DENV and ZIKV isolates. Although the precise reason for high cross-reactivity between viruses is unknown, possible mechanisms may include antibodies that interact with additional quaternary and glycosylated epitopes that were not present on the recombinant antigens, or other indeterminate factors (14, 62). Further, the results presented here emphasize the value of determining total antibody recognition of E proteins for distinguishing between infections caused by different species of flaviviruses. While virus neutralization assays measure a functional subset of antibodies and provide an important indicator of anti-viral immunity, the best correlate of protection against viremia in DENV infection may be total polyclonal antibodies rather than neutralizing antibody titers (49). Antibodies that are weakly neutralizing in cell culture assays can contribute to physiologically important non-ADE mechanisms of virus clearance that are facilitated by receptor-mediated uptake and effector cells (63).

Clinical and Vaccine Immunology

A more detailed understanding of the interrelationships of antibody responses across flaviviruses is imperative because infections by one species or serotype are known to influence disease susceptibility and severity for infections caused by other related viruses (25-28). New techniques are also needed to guide accurate diagnosis of emerging infections, especially for flavivirus-immune individuals, as antibodies persist at levels that are detectable long after disease resolution (52, 58, 64, 65). Although the lapse of time from previous exposures may influence detection of responses to new infections, our results demonstrate that antibody recognition patterns from secondary infections can be used to estimate infection histories (Fig. 6). Importantly, since severe dengue is linked to secondary infections with a heterotypic DENV (25-28), it is possible that dengue-primed populations are more prone to ZIKV infections, and perhaps the associated severe neurological disorders of Guillain-Barré syndrome (8) and microcephaly (4-6). However, there is currently no evidence of enhanced severity, increased ZIKV loads, or increased incidence of Zika disease in countries with wide-spread immunity to dengue. Our results indicate that it should be possible to develop protein-based serological assays that are sensitive enough to differentiate flavivirus infections in individuals with preexisting immunity. Based on the assumption that multiple independent antibody-binding events were measured for each clinical specimen collected from a dengue-endemic region, data from primary infections can be used to train machine learning methods for classification of sera from unknown infection histories. The predictive algorithm that we developed for E recognition patterns may find useful applications in disease surveillance for inference of infection histories in both primary and secondary flavivirus encounters. As diagnostic methods by necessity focus only on the current disease, the general approach described here will also be important for addressing any causal relationships between Zika disease and previous infections.

527

528 **End Notes**

529 Author contributions: R. G. U., C. L. P., S. L. K., J. L. S. and S. M. R. J. designed the study; D.
530 M. D., A. P. D. collected and organized sera; C. L. P., J. L. S. and S. M. R. J. performed the
531 experiments; S. L. K., C. L. P., J. L. S., S. M. R. J., D. H. O., R. D. H. and R. G. U. analyzed the
532 data; S. L. K., C. L. P., J. L. S., S. M. R. J. and R. G. U. wrote the manuscript; all authors
533 reviewed and edited the manuscript.

534

535 The authors acknowledge grant support from NIAID to R. G. U. (R01AI096215) and D. H. O.
536 (R01AI116382-01A1). This research was supported in part by an appointment of S.L.K. to the
537 Postgraduate Research Participation Program administered by Oak Ridge Institute for Science
538 and Education through an interagency agreement with the U.S. Department of Energy.
539 The authors thank Andrew Haddow, USAMRIID, for supplying many of the ZIKV strains used
540 in this study, Julia S. Ampuero, Carolina Guevara, NAMRU-6, Lima, Peru, and the staff of
541 DIRESA Loreto for collection and analysis of human disease sera, and also Veterinary, Animal
542 Care, Scientific Protocol Implementation, and the Pathology staff at the Wisconsin National
543 Primate Research Center (WNPRC) for their contributions to this study. Opinions,
544 interpretations, conclusions, and recommendations are those of the authors and are not
545 necessarily endorsed by any branch of the U.S. government.
546 The authors declare that they have no competing interests.

547

548

549

References

1. **Ferreira-de-Brito A, Ribeiro IP, Miranda RM, Fernandes RS, Campos SS, Silva KA, Castro MG, Bonaldo MC, Brasil P, Lourenco-de-Oliveira R.** 2016. First detection of natural infection of Aedes aegypti with Zika virus in Brazil and throughout South America. Memorias do Instituto Oswaldo Cruz **111:**655-658.
2. **Vasilakis N, Weaver SC.** 2016. Flavivirus transmission focusing on Zika. Current opinion in virology **22:**30-35.
3. **Musso D, Roche C, Robin E, Nhan T, Teissier A, Cao-Lormeau VM.** 2015. Potential sexual transmission of Zika virus. Emerging infectious diseases **21:**359-361.
4. **Cauchemez S, Besnard M, Bompard P, Dub T, Guillemette-Artur P, Eyrolle-Guignot D, Salje H, Van Kerkhove MD, Abadie V, Garel C, Fontanet A, Mallet HP.** 2016. Association between Zika virus and microcephaly in French Polynesia, 2013-15: a retrospective study. Lancet **387:**2125-2132.
5. **Schuler-Faccini L, Ribeiro EM, Feitosa IM, Horovitz DD, Cavalcanti DP, Pessoa A, Doriqui MJ, Neri JI, Neto JM, Wanderley HY, Cernach M, El-Husny AS, Pone MV, Serao CL, Sanseverino MT, Brazilian Medical Genetics Society-Zika Embryopathy Task F.** 2016. Possible Association Between Zika Virus Infection and Microcephaly - Brazil, 2015. MMWR. Morbidity and mortality weekly report **65:**59-62.
6. **Rasmussen SA, Jamieson DJ, Honein MA, Petersen LR.** 2016. Zika Virus and Birth Defects--Reviewing the Evidence for Causality. The New England journal of medicine **374:**1981-1987.
7. **Lazear HM, Diamond MS.** 2016. Zika Virus: New Clinical Syndromes and Its Emergence in the Western Hemisphere. Journal of virology **90:**4864-4875.
8. **Cao-Lormeau VM, Blake A, Mons S, Lastere S, Roche C, Vanhomwegen J, Dub T, Baudouin L, Teissier A, Larre P, Vial AL, Decam C, Choumet V, Halstead SK, Willison HJ, Musset L, Manuguerra JC, Despres P, Fournier E, Mallet HP, Musso D, Fontanet A, Neil J, Ghawche F.** 2016. Guillain-Barre Syndrome outbreak associated with Zika virus infection in French Polynesia: a case-control study. Lancet **387:**1531-1539.
9. **Duffy MR, Chen TH, Hancock WT, Powers AM, Kool JL, Lanciotti RS, Pretrick M, Marfel M, Holzbauer S, Dubray C, Guillaumot L, Griggs A, Bel M, Lambert AJ, Laven J, Kosoy O, Panella A, Biggerstaff BJ, Fischer M, Hayes EB.** 2009. Zika virus outbreak on Yap Island, Federated States of Micronesia. The New England journal of medicine **360:**2536-2543.
10. **Ioos S, Mallet HP, Leparc Goffart I, Gauthier V, Cardoso T, Herida M.** 2014. Current Zika virus epidemiology and recent epidemics. Medecine et maladies infectieuses **44:**302-307.
11. **Musso D, Gubler DJ.** 2016. Zika Virus. Clinical microbiology reviews **29:**487-524.
12. **Kindhauser MK, Allen T, Frank V, Santhana RS, Dye C.** 2016. Zika: the origin and spread of a mosquito-borne virus. Bulletin of the World Health Organization **94:**675-686C.
13. **Kostyuchenko VA, Lim EX, Zhang S, Fibriansah G, Ng TS, Ooi JS, Shi J, Lok SM.** 2016. Structure of the thermally stable Zika virus. Nature **533:**425-428.

14. **Sirohi D, Chen Z, Sun L, Klose T, Pierson TC, Rossmann MG, Kuhn RJ.** 2016. The 3.8 A resolution cryo-EM structure of Zika virus. Science **352:**467-470.
15. **Zhang X, Ge P, Yu X, Brannan JM, Bi G, Zhang Q, Schein S, Zhou ZH.** 2013. Cryo-EM structure of the mature dengue virus at 3.5-A resolution. Nature structural & molecular biology **20:**105-110.
16. **Mukhopadhyay S, Kim BS, Chipman PR, Rossmann MG, Kuhn RJ.** 2003. Structure of West Nile virus. Science **302:**248.
17. **Rey FA, Heinz FX, Mandl C, Kunz C, Harrison SC.** 1995. The envelope glycoprotein from tick-borne encephalitis virus at 2 A resolution. Nature **375:**291-298.
18. **Luca VC, AbiMansour J, Nelson CA, Fremont DH.** 2012. Crystal structure of the Japanese encephalitis virus envelope protein. Journal of virology **86:**2337-2346.
19. **Lok SM.** 2016. The Interplay of Dengue Virus Morphological Diversity and Human Antibodies. Trends in microbiology **24:**284-293.
20. **Aliota MT, Dudley DM, Newman CM, Mohr EL, Gellerup DD, Breitbach ME, Buechler CR, Rasheed MN, Mohns MS, Weiler AM, Barry GL, Weisgrau KL, Eudailey JA, Rakasz EG, Vosler LJ, Post J, Capuano S, 3rd, Golos TG, Permar SR, Osorio JE, Friedrich TC, O'Connor SL, O'Connor DH.** 2016. Heterologous Protection against Asian Zika Virus Challenge in Rhesus Macaques. PLoS neglected tropical diseases **10:**e0005168.
21. **Dai L, Song J, Lu X, Deng YQ, Musyoki AM, Cheng H, Zhang Y, Yuan Y, Song H, Haywood J, Xiao H, Yan J, Shi Y, Qin CF, Qi J, Gao GF.** 2016. Structures of the Zika Virus Envelope Protein and Its Complex with a Flavivirus Broadly Protective Antibody. Cell host & microbe **19:**696-704.
22. **Stettler K, Beltramello M, Espinosa DA, Graham V, Cassotta A, Bianchi S, Vanzetta F, Minola A, Jaconi S, Mele F, Foglierini M, Pedotti M, Simonelli L, Dowall S, Atkinson B, Percivalle E, Simmons CP, Varani L, Blum J, Baldanti F, Cameroni E, Hewson R, Harris E, Lanzavecchia A, Sallusto F, Corti D.** 2016. Specificity, cross-reactivity, and function of antibodies elicited by Zika virus infection. Science **353:**823-826.
23. **Song H, Qi J, Haywood J, Shi Y, Gao GF.** 2016. Zika virus NS1 structure reveals diversity of electrostatic surfaces among flaviviruses. Nature structural & molecular biology **23:**456-458.
24. **Calisher CH, Karabatsos N, Dalrymple JM, Shope RE, Porterfield JS, Westaway EG, Brandt WE.** 1989. Antigenic relationships between flaviviruses as determined by cross-neutralization tests with polyclonal antisera. The Journal of general virology **70 (Pt 1):**37-43.
25. **Anderson KB, Gibbons RV, Thomas SJ, Rothman AL, Nisalak A, Berkelman RL, Libraty DH, Endy TP.** 2011. Preexisting Japanese encephalitis virus neutralizing antibodies and increased symptomatic dengue illness in a school-based cohort in Thailand. PLoS neglected tropical diseases **5:**e1311.
26. **Reisen WK, Lothrop HD, Wheeler SS, Kennsington M, Gutierrez A, Fang Y, Garcia S, Lothrop B.** 2008. Persistent West Nile virus transmission and the apparent displacement St. Louis encephalitis virus in southeastern California, 2003-2006. Journal of medical entomology **45:**494-508.

Clinical and Vaccine Immunology

27. **Kliks SC, Nimmanitya S, Nisalak A, Burke DS.** 1988. Evidence that maternal dengue antibodies are important in the development of dengue hemorrhagic fever in infants. The American journal of tropical medicine and hygiene **38:**411-419.
28. **Halstead SB, Marchette NJ, Sung Chow JS, Lolekha S.** 1976. Dengue virus replication enhancement in peripheral blood leukocytes from immune human beings. Proceedings of the Society for Experimental Biology and Medicine. Society for Experimental Biology and Medicine **151:**136-139.
29. **Halstead SB, Rojanasuphot S, Sangkawibha N.** 1983. Original antigenic sin in dengue. The American journal of tropical medicine and hygiene **32:**154-156.
30. **Russell PK, Udomsakdi S, Halstead SB.** 1967. Antibody response in dengue and dengue hemorrhagic fever. Japanese journal of medical science & biology **20 Suppl:**103-108.
31. **Lanciotti RS, Kosoy OL, Laven JJ, Velez JO, Lambert AJ, Johnson AJ, Stanfield SM, Duffy MR.** 2008. Genetic and serologic properties of Zika virus associated with an epidemic, Yap State, Micronesia, 2007. Emerging infectious diseases **14:**1232-1239.
32. **CDC** 2016, posting date. Revised dianostic testing for Zika, chikungunya, and dengue viruses in US public health laboratories. [Online.]
33. **Dudley DM, Aliota MT, Mohr EL, Weiler AM, Lehrer-Brey G, Weisgrau KL, Mohns MS, Breitbach ME, Rasheed MN, Newman CM, Gellerup DD, Moncla LH, Post J, Schultz-Darken N, Schotzko ML, Hayes JM, Eudailey JA, Moody MA, Permar SR, O'Connor SL, Rakasz EG, Simmons HA, Capuano S, Golos TG, Osorio JE, Friedrich TC, O'Connor DH.** 2016. A rhesus macaque model of Asian-lineage Zika virus infection. Nature communications **7:**12204.
34. **Tan JL, Lok SM.** 2014. Dengue virus purification and sample preparation for cryo-electron microscopy. Methods in molecular biology **1138:**41-52.
35. **Krogh A, Larsson B, von Heijne G, Sonnhammer EL.** 2001. Predicting transmembrane protein topology with a hidden Markov model: application to complete genomes. Journal of molecular biology **305:**567-580.
36. **Sonnhammer EL, von Heijne G, Krogh A.** 1998. A hidden Markov model for predicting transmembrane helices in protein sequences. Proceedings / ... International Conference on Intelligent Systems for Molecular Biology ; ISMB. International Conference on Intelligent Systems for Molecular Biology **6:**175-182.
37. **Nallamsetty S, Austin BP, Penrose KJ, Waugh DS.** 2005. Gateway vectors for the production of combinatorially-tagged His6-MBP fusion proteins in the cytoplasm and periplasm of Escherichia coli. Protein science : a publication of the Protein Society **14:**2964-2971.
38. **Palmer I, Wingfield PT.** 2012. Preparation and extraction of insoluble (inclusion-body) proteins from Escherichia coli. Current protocols in protein science / editorial board, John E. Coligan ... [et al.] **Chapter 6:**Unit6 3.
39. **Saeed AI, Sharov V, White J, Li J, Liang W, Bhagabati N, Braisted J, Klapa M, Currier T, Thiagarajan M, Sturn A, Snuffin M, Rezantsev A, Popov D, Ryltsov A, Kostukovich E, Borisovsky I, Liu Z, Vinsavich A, Trush V, Quackenbush J.** 2003. TM4: a free, open-source system for microarray data management and analysis. BioTechniques **34:**374-378.

Clinical and Vaccine Immunology

40. **Meyer D., Dimitriadou E., Hornik K., Weingessel A., Leisch F., Chang C., Lin C.** 2015. Support Vector Machines, Misc Functions of the Department of Statistics, Probability Theory Group (Formerly: E1071), TU Wien, August 5, 2015 ed.
41. **Larkin MA, Blackshields G, Brown NP, Chenna R, McGettigan PA, McWilliam H, Valentin F, Wallace IM, Wilm A, Lopez R, Thompson JD, Gibson TJ, Higgins DG.** 2007. Clustal W and Clustal X version 2.0. Bioinformatics **23:**2947-2948.
42. **Di Tommaso P, Moretti S, Xenarios I, Orobitg M, Montanyola A, Chang JM, Taly JF, Notredame C.** 2011. T-Coffee: a web server for the multiple sequence alignment of protein and RNA sequences using structural information and homology extension. Nucleic acids research **39:**W13-17.
43. **Notredame C, Higgins DG, Heringa J.** 2000. T-Coffee: A novel method for fast and accurate multiple sequence alignment. Journal of molecular biology **302:**205-217.
44. **Castresana J.** 2000. Selection of conserved blocks from multiple alignments for their use in phylogenetic analysis. Molecular biology and evolution **17:**540-552.
45. **Talavera G, Castresana J.** 2007. Improvement of phylogenies after removing divergent and ambiguously aligned blocks from protein sequence alignments. Systematic biology **56:**564-577.
46. **Guindon S, Dufayard JF, Lefort V, Anisimova M, Hordijk W, Gascuel O.** 2010. New algorithms and methods to estimate maximum-likelihood phylogenies: assessing the performance of PhyML 3.0. Systematic biology **59:**307-321.
47. 2016, posting date. Zika Open-Research Portal. [Online.]
48. **Fernandez S, Cisney ED, Tikhonov AP, Schweitzer B, Putnak RJ, Simmons M, Ulrich RG.** 2011. Antibody recognition of the dengue virus proteome and implications for development of vaccines. Clinical and vaccine immunology : CVI **18:**523-532.
49. **Simmons M, Burgess T, Lynch J, Putnak R.** 2010. Protection against dengue virus by non-replicating and live attenuated vaccines used together in a prime boost vaccination strategy. Virology **396:**280-288.
50. **Larsen CP, Whitehead SS, Durbin AP.** 2015. Dengue human infection models to advance dengue vaccine development. Vaccine **33:**7075-7082.
51. **Kirkpatrick BD, Whitehead SS, Pierce KK, Tibery CM, Grier PL, Hynes NA, Larsson CJ, Sabundayo BP, Talaat KR, Janiak A, Carmolli MP, Luke CJ, Diehl SA, Durbin AP.** 2016. The live attenuated dengue vaccine TV003 elicits complete protection against dengue in a human challenge model. Science translational medicine **8:**330ra336.
52. **Durieux C.** 1956. Mass yellow fever vaccination in French Africa South of Sahara., p. 115-121. *In* Smithburn KC, Durieux, C., Koerber, R., Panna, H. A., Dick, G. W. A., Courtois, G., de Sousa Manso, C., Stuart, G., Bonnel, P. H. (ed.), Yellow Fever Vaccination. Geneva.
53. 2012, posting date. Viral and Immune parameters of Dengue and WNV in donors: Blood safety implications. [Online.]
54. **Ramos HJ, Lanteri MC, Blahnik G, Negash A, Suthar MS, Brassil MM, Sodhi K, Treuting PM, Busch MP, Norris PJ, Gale M, Jr.** 2012. IL-1beta signaling promotes CNS-intrinsic immune control of West Nile virus infection. PLoS pathogens **8:**e1003039.
55. **Haddow AD, Schuh AJ, Yasuda CY, Kasper MR, Heang V, Huy R, Guzman H, Tesh RB, Weaver SC.** 2012. Genetic characterization of Zika virus strains: geographic expansion of the Asian lineage. PLoS neglected tropical diseases **6:**e1477.

56. **Dowd KA, DeMaso CR, Pelc RS, Speer SD, Smith AR, Goo L, Platt DJ, Mascola JR, Graham BS, Mulligan MJ, Diamond MS, Ledgerwood JE, Pierson TC.** 2016. Broadly Neutralizing Activity of Zika Virus-Immune Sera Identifies a Single Viral Serotype. Cell reports **16:**1485-1491.

57. **VanBlargan LA, Mukherjee S, Dowd KA, Durbin AP, Whitehead SS, Pierson TC.** 2013. The type-specific neutralizing antibody response elicited by a dengue vaccine candidate is focused on two amino acids of the envelope protein. PLoS pathogens **9:**e1003761.

58. **Monath T CM, Teuwen DE.** 2008. Yellow fever vaccine, p. 959-1055. *In* Plotkin SA OW, Offit PA (ed.), Vaccines, 5th ed. Saunders Elsevier, Philadelphia, PA.

59. **Dejnirattisai W, Supasa P, Wongwiwat W, Rouvinski A, Barba-Spaeth G, Duangchinda T, Sakuntabhai A, Cao-Lormeau VM, Malasit P, Rey FA, Mongkolsapaya J, Screaton GR.** 2016. Dengue virus sero-cross-reactivity drives antibody-dependent enhancement of infection with zika virus. Nature immunology **17:**1102-1108.

60. **St George K, Sohi IS, Dufort EM, Dean AB, White JL, Limberger R, Sommer JN, Ostrowski S, Wong SJ, Backenson PB, Kuhles D, Blog D, Taylor J, Hutton B, Zucker HA.** 2017. Zika Virus Testing Considerations: Lessons Learned from the First 80 Real-Time Reverse Transcription-PCR-Positive Cases Diagnosed in New York State. Journal of clinical microbiology **55:**535-544.

61. **Priyamvada L, Cho A, Onlamoon N, Zheng NY, Huang M, Kovalenkov Y, Chokephaibulkit K, Angkasekwinai N, Pattanapanyasat K, Ahmed R, Wilson PC, Wrammert J.** 2016. B Cell Responses during Secondary Dengue Virus Infection Are Dominated by Highly Cross-Reactive, Memory-Derived Plasmablasts. Journal of virology **90:**5574-5585.

62. **Dejnirattisai W, Wongwiwat W, Supasa S, Zhang X, Dai X, Rouvinski A, Jumnainsong A, Edwards C, Quyen NT, Duangchinda T, Grimes JM, Tsai WY, Lai CY, Wang WK, Malasit P, Farrar J, Simmons CP, Zhou ZH, Rey FA, Mongkolsapaya J, Screaton GR.** 2015. A new class of highly potent, broadly neutralizing antibodies isolated from viremic patients infected with dengue virus. Nature immunology **16:**170-177.

63. **Klasse PJ.** 2014. Neutralization of Virus Infectivity by Antibodies: Old Problems in New Perspectives. Advances in biology **2014**.

64. **Prince HE, Tobler LH, Yeh C, Gefter N, Custer B, Busch MP.** 2007. Persistence of West Nile virus-specific antibodies in viremic blood donors. Clinical and vaccine immunology : CVI **14:**1228-1230.

65. **Roehrig JT, Nash D, Maldin B, Labowitz A, Martin DA, Lanciotti RS, Campbell GL.** 2003. Persistence of virus-reactive serum immunoglobulin m antibody in confirmed west nile virus encephalitis cases. Emerging infectious diseases **9:**376-379.

766 **Figure Legends**

767 **Figure 1. Phylogenetic relationships and recognition of microarrayed antigens by virus-**
768 **specific antibody standards.** (**A**) The phylogenies of flaviviruses examined in this study were
769 inferred from an alignment of amino acid sequences from envelope (E) proteins. (**B**) Microarrays
770 of E, non-structural 1 (NS1), and membrane (pM) proteins probed with mouse polyclonal
771 antibodies generated against each virus shown (centered labels above each bar graph). Antibody
772 binding data are shown as log10-transformed mean fluorescence intensity (± SEM), and arrows
773 (↓) indicate the virus-specific antigens. Heterologous antigens that exhibit increased recognition
774 compared to the virus-specific antigen are labeled with * ($p < 0.05$, one-way ANOVA with
775 Tukey's range test). YFV, yellow fever virus; SLEV, St. Louis encephalitis virus; DENV (1-4),
776 dengue virus; POWV, Powassan virus; TBEV, tick-borne encephalitis virus; MVEV, Murray
777 Valley encephalitis virus; WNV, West Nile virus; ZIKV, Zika virus; JEV, Japanese encephalitis
778 virus; ROCV, Rocio virus.
779
780 **Figure 2. Specificity and kinetics of the humoral immune response to ZIKV.**
781 ZIKV-challenged non-human primate (NHP) IgG recognition of ZIKV particles harvested early
782 (**A**, left, 48 h) or late (**A**, right, 144 h) post-infection of HEK293T cells, and ZIKV proteins (**B**;
783 envelope, E; nonstructural protein 1, NS1; premembrane protein, pM), from five Asian (AS) and
784 six African (AFR) lineages (Table 1). ZIKV-specific antibody responses are denoted by scatter
785 plots with center horizontal lines representing the mean binding of serum antibodies from NHPs
786 challenged with either an AFR- (n=3, circles) or AS- (n = 3, squares) lineage ZIKV at 0-2 days
787 post-infection (DPI; open symbols) and 21-28 DPI (filled symbols). Error bars indicate ± SEM.
788 Statistically significant differences between mean antibody binding of all ZIKV-challenged

NHPs to ZIKV antigens at 0-2 DPI and 21-28 DPI were calculated using a one-tailed Student's t-test (*, $p < 7.5e-5$; ns, not significant), while no significant differences were observed between mean antibody binding of ZIKV-AS- and ZIKV-AFR-challenged groups to AS and AFR ZIKV antigens at 21-28 DPI (two-tailed Student's t-test). (**C**) IgM (green) and IgG (orange) binding profiles to ZIKV particles (144 h harvest) (top) and ZIKV E protein (bottom) are compared to viral load (47) (black) from pre-infection (day 0) to 28 DPI for ZIKV-challenged NHPs (n = 9). Second- (IgM), third- (IgG) and fourth- (viral load) order polynomial curves were fitted to the data, with fitted lines and shading under the curve consistent with data point colors.

Figure 3. Differentiation of non-human primates challenged with ZIKV or DENV by specific IgG binding to E antigens. (**A**) Binding of convalescent serum antibodies from non-human primates (NHP) challenged with either an Asian (H/PF, red, n = 3) or African (MR-766, royal blue, n = 3) –lineage ZIKV, or DENV (n = 4 each for DENV1, black; DENV2, green; DENV3, orange; and n = 3 for DENV4, magenta) to whole viruses (144 h, left) and E proteins (right). Values shown are antibody binding signals relative to the virus used for challenge (± SEM). (**B**) Principal component analyses of relative IgG binding to E proteins (left) and viruses (144 h, right) by NHP antibodies. Individual data points and virus-specific clusters are colored according to challenge virus as in **A**.

Figure 4. Antibody specificity of primary and secondary flavivirus infections. Relative binding (± SEM) of convalescent serum antibodies from non-human primate (NHP) and human flavivirus infections to fifteen flavivirus E proteins. (**A**) Sera from primary infections: grey, DENV-challenged NHPs (individual data from each NHP is overlaid in a scatter plot: n = 4 each

for DENV1, black; DENV2, green; DENV3, orange; and n = 3 for DENV4, magenta); green, human rDEN2Δ30 (n = 8); red, pooled African and Asian-lineage ZIKV NHPs (n = 6); white, YFV-vaccinated NHPs (n = 3). (**B**) Sera from confirmed human flaviviral infections with unknown infection histories: grey, DENV (individual data is overlaid in a scatter plot and colors correspond to most recent DENV infection: DENV2, green (n = 5); DENV3, orange (n = 2)); red, ZIKV (n = 4); white, YFV vaccination (n = 13); cyan, WNV (n = 20). (**C**) Predicted infection histories of human secondary DENV (**B**, grey) and primary ZIKV (**B**, red) infections, based on a supervised SVM classifier. Individual human sera are shown at the bottom (Z, ZIKV; D2, DENV2; D3, DENV3; followed by sera identification (ID) number), with probability values for each viral class (left) gradient colored from low to high (white – royal blue, right). Predicted infection histories are designated by colored bar above sera ID (DENV1, black; DENV4, magenta; no prediction, unfilled).

Figure 5. Quantitative comparisons of antibodies directed to the infecting virus versus all other flaviviruses. Antibody recognition of microarrayed E proteins displayed as mean fluorescence intensity (± SEM). Antibodies from primary flavivirus infections of NHPs (ZIKV, DENV1-4, YFV) and humans (rDEN2Δ30) exhibited significantly decreased recognition of heterologous E antigens compared to virus-specific E (dark grey) ($p < 0.05$, one-way ANOVA with Tukey's range test). DENV E proteins (light gray) are separated from all other flavivirus E proteins (white, inclusive of YFV, SLEV, POWV, TBEV, MVEV, WNV, JEV, ROCV) to show DENV antibody cross-reactivity between serotypes.

Figure 6. Overlap in rising and waning antibody responses to independent infections. The primary infection of a flavivirus-naïve individual with dengue virus occurs at day 0 (solid black arrowhead). Levels of virus-specific antibody (gray bars and shading) begin to increase shortly after the acute phase of infection, peak after convalescence, and subside thereafter. A second infection with Zika virus (solid red arrowhead) is followed by an increase in virus-specific antibody (red bars and shading), resulting in detection of a mixture of anti-dengue and anti-Zika virus antibodies that will vary with time from infections. The ratio of dengue : Zika virus antibodies, as shown, will be further increased if the secondary infection results in a less potent activation of serological immune responses.

Table 1. Flavivirus strains used for production of whole viruses and recombinant proteins.

Virus	ID[a]	Isolate	Country	Year	Host	Acc. No.
ZIKV Asian lineage		H/PF/2013[b]	French Polynesia	2013	Human	KJ776791
	1	SV0127/14	Thailand	2014	Human	KU681081
	2	CPC-0740[c]	Philippines	2012	Human	KU681082
	3	VABC59	Puerto Rico	2015	Human	KU501215
	4	SPH2015	Brazil	2015	Human	KU321639
	5	YAP[c]	Micronesia	2007	Human	EU545988
ZIKV African lineage	1	MR-766[b,c]	Uganda	1947	*Mucaca mulatta*	KU955594
	2	IBH30656	Nigeria	1968	Human	HQ234500
	3	DAKAR41525	Senegal	1984	*Aedes africanus*	KU955591
	4	DAKAR 41662	Senegal	1984	*A. africanus*	KU955592
	5	ARB7701	Central Africa	1976	*A. africanus*	KF268950
	6	ArD_41519	Senegal	1984	*A. africanus*	HQ234501
DENV1		HAWAII	USA	1944	Human	KM204119
DENV2		NGC	New Guinea	1944	Human	KM204118
DENV3		H87	Philippines	1956	Human	M93130
DENV4		H241	Philippines	1956	Human	AY947539
WNV		NY99	USA	1999	Owl	NC_009942
YFV		17-D-204	USA	1985	Vaccine	JX503529
JEV		SA14-14-2	South Korea	2006	Vaccine	JN604986
SLEV		PARTON	USA	1933	Human	EF158070
MVEV		1-51	Australia	1952	Human	NC_000943
ROCV		SPH34675	Brazil	1975	Human	AY632542
POWV		LB	Canada	1958	Human	NC_003687
TBEV-E		SOFJIN-HO	Russia	1937	Human	AB062064
TBEV-EUR		NEUDOERFL	Austria	1971	*Ixodes ricinus*	NC_001672

[a]ID corresponds to ZIKV strain labels shown in Fig. 2A and B.
[b]Used for challenge of *M. mulatta*.
[c]Representative antigens shown in Fig. 2C-4 and Supplementary Fig. 2-4 (virus, CPC-0740; YAP, E protein).
Virus abbreviations: Zika (ZIKV), dengue (DENV), West Nile (WNV), yellow fever (YFV), Japanese encephalitis (JEV), St. Louis encephalitis (SLEV), Murray Valley encephalitis (MVEV), rocio (ROCV), Powassan (POWV), tick-borne encephalitis (TBEV).

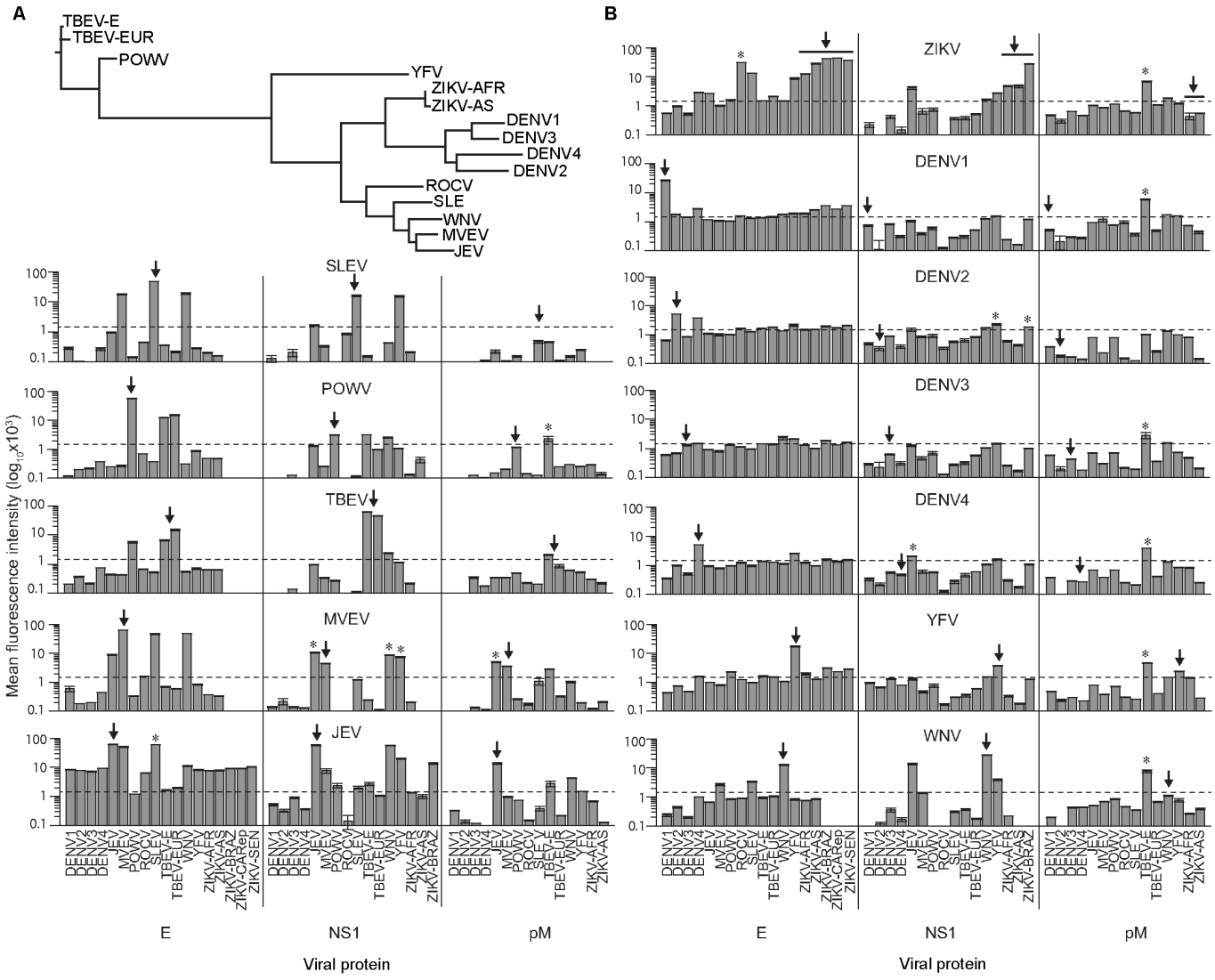

Figure 1

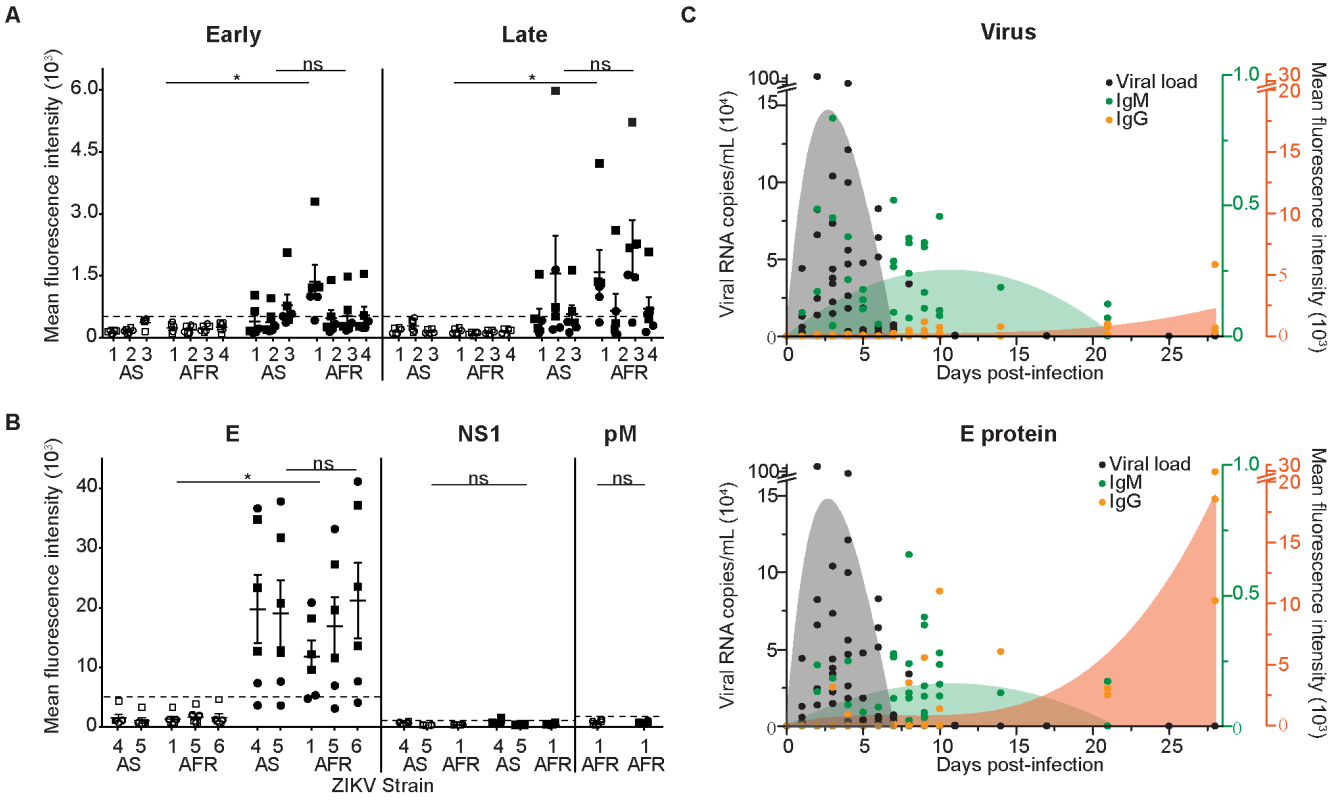

Figure 2

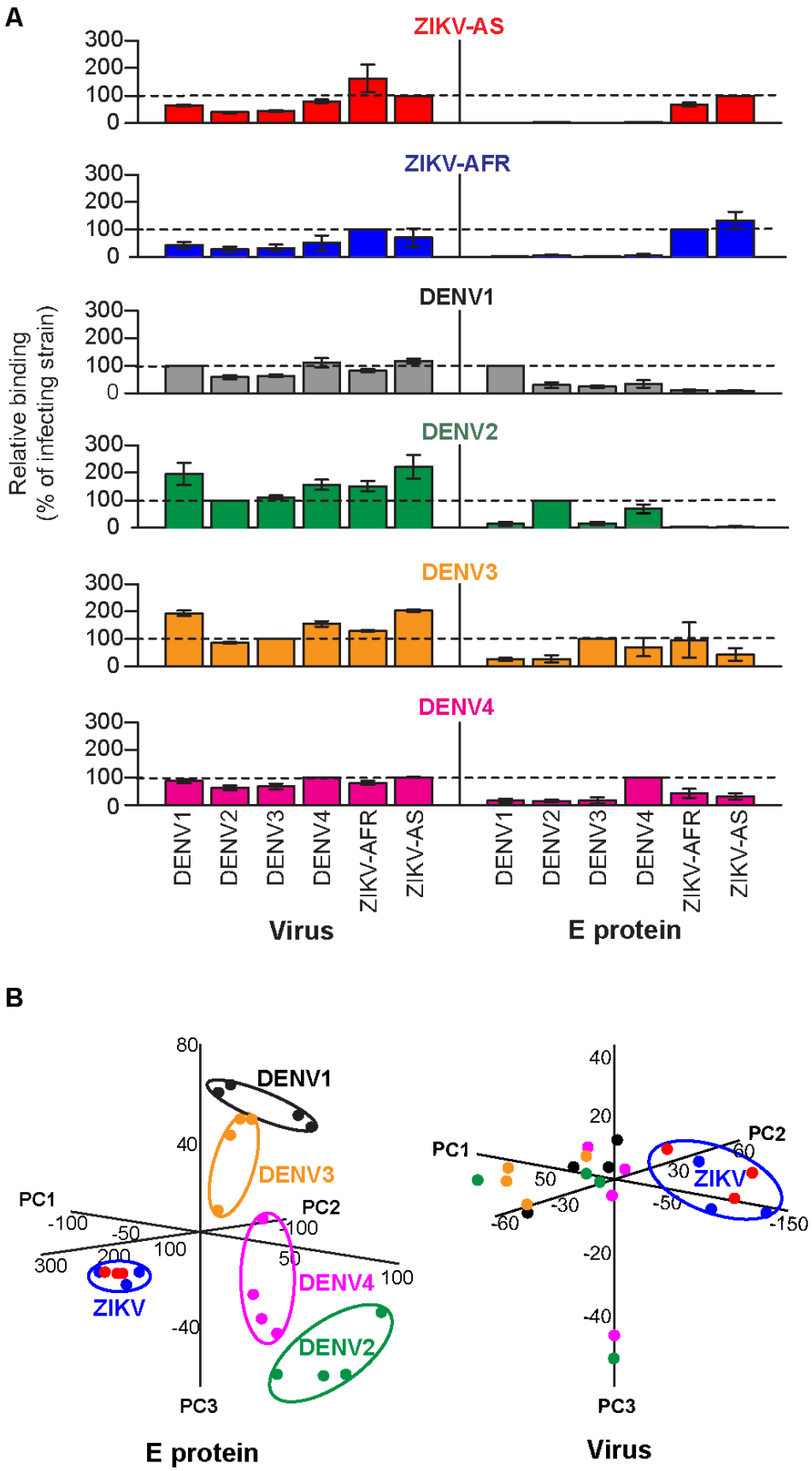

Figure 3

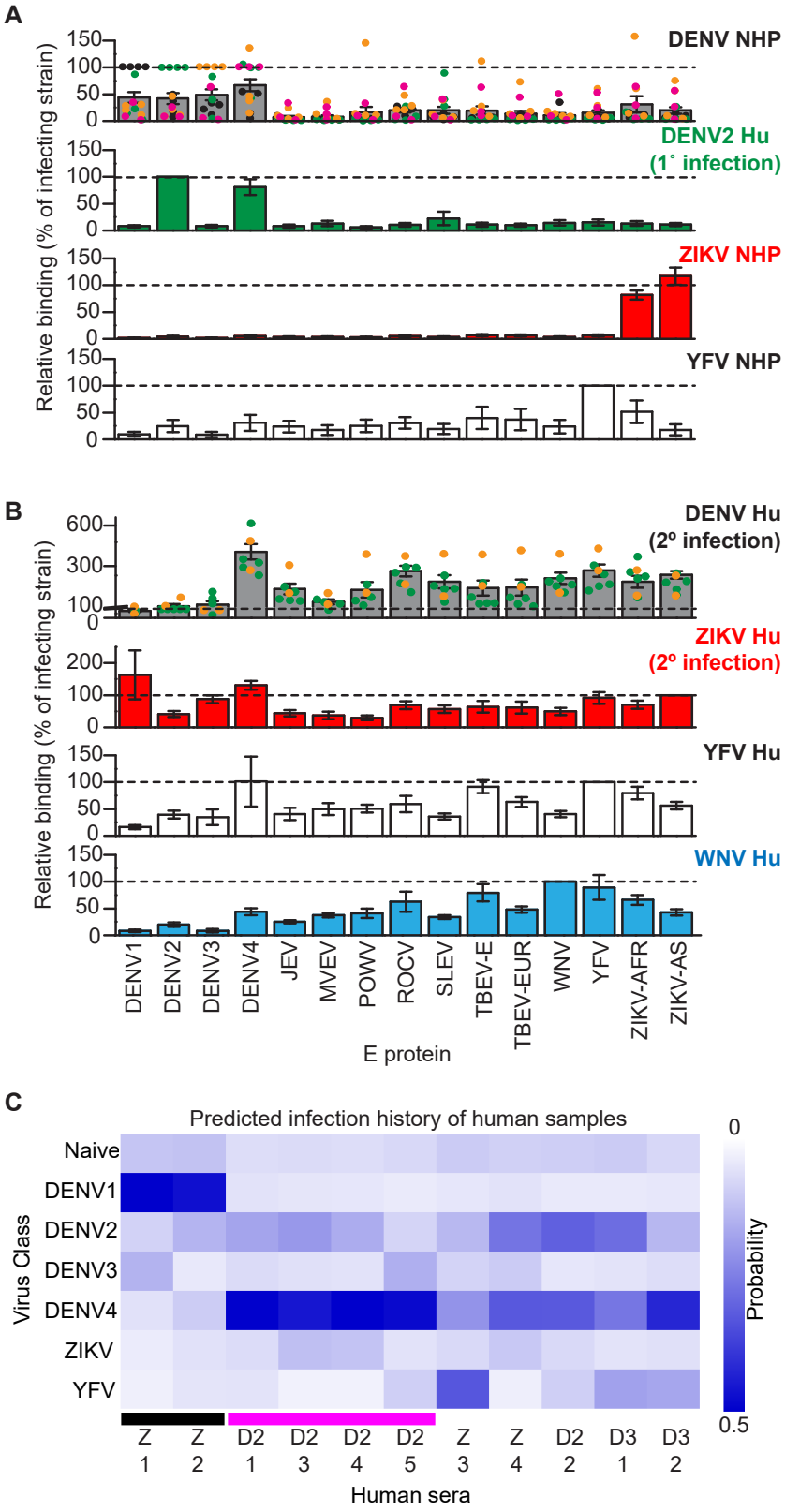

Figure 4

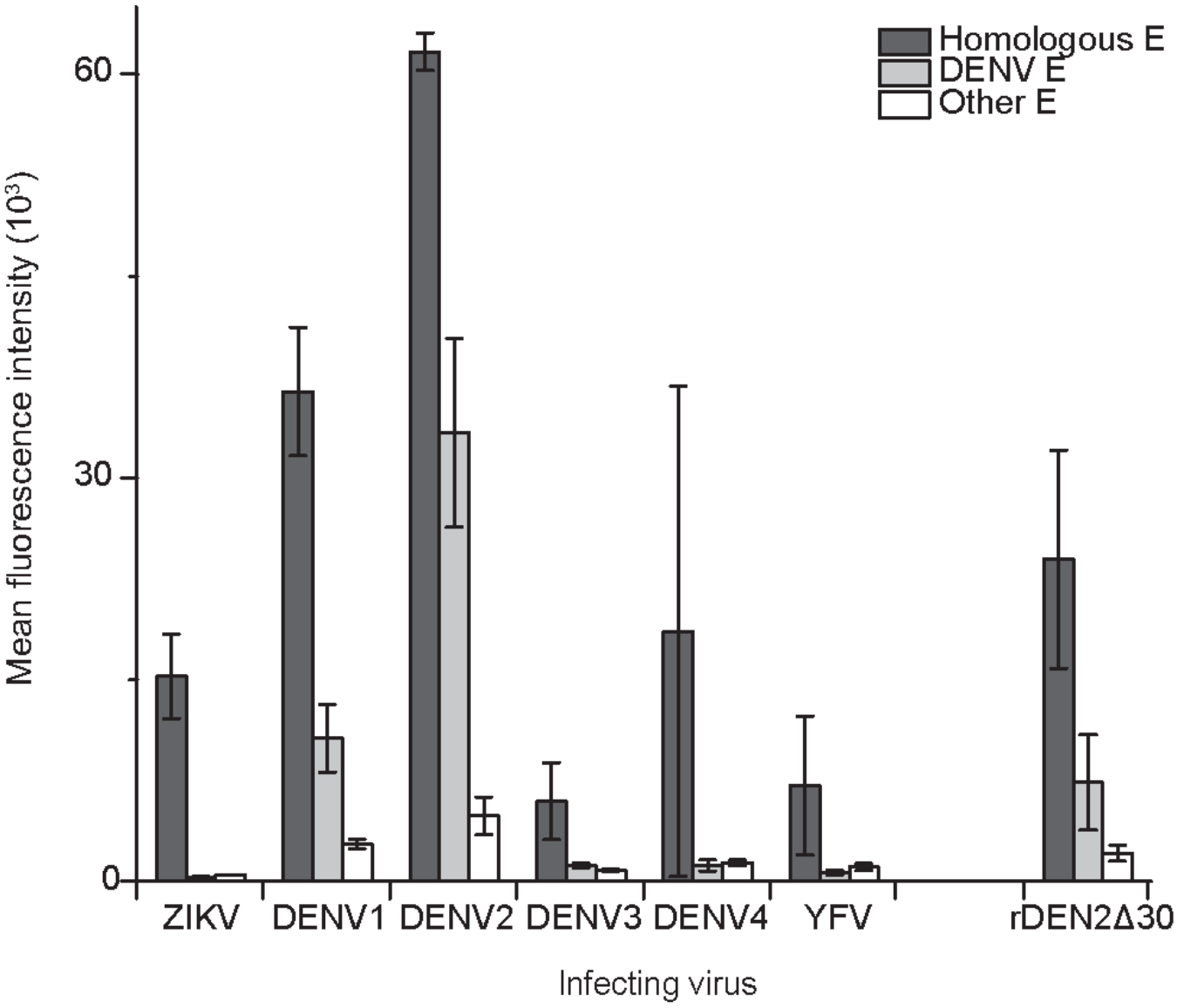

Figure 5

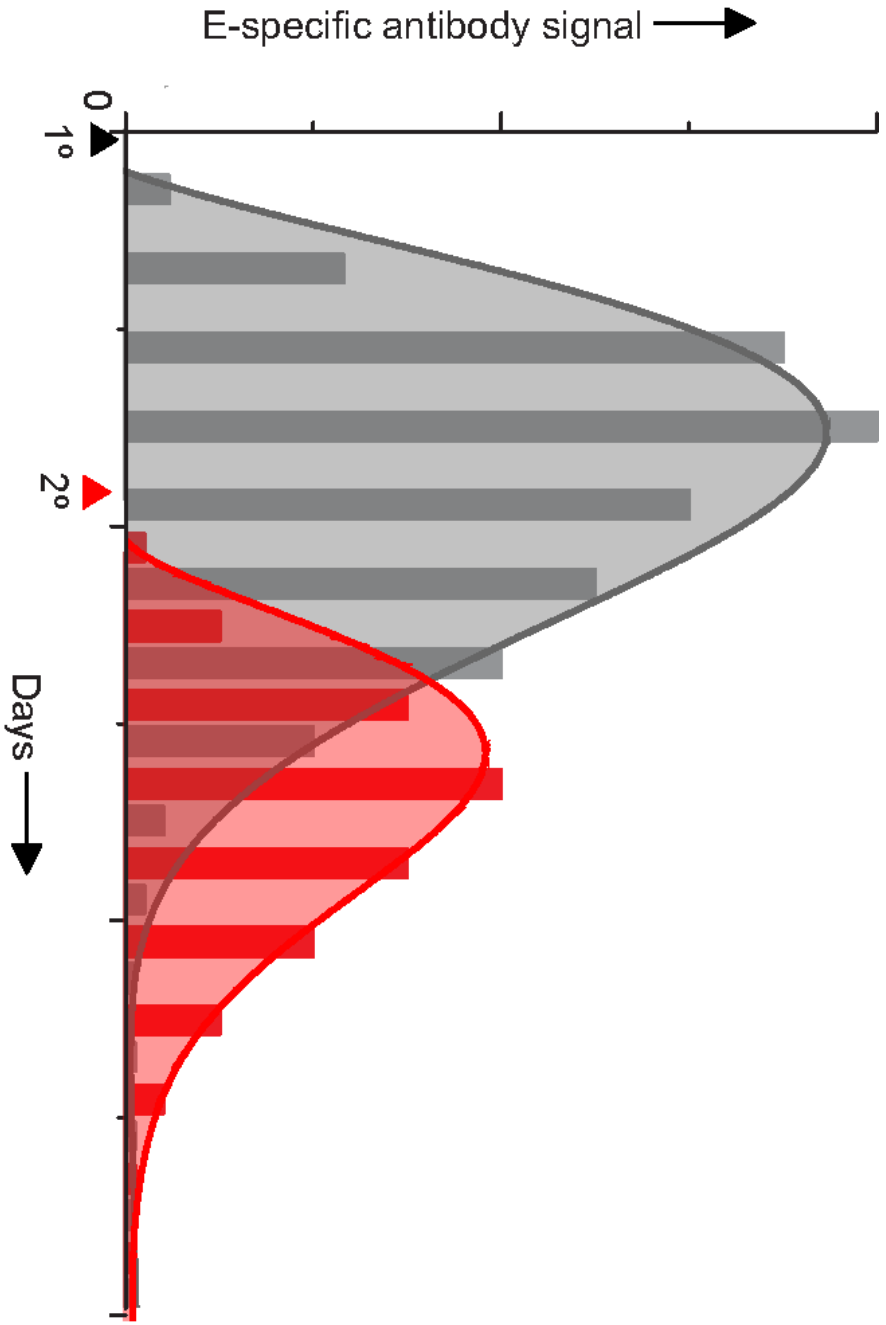

Figure 6